









Multicore-Fiber Receptacle With Compact Fan-In/Fan-Out Device for SDM Transceiver Applications

Kota Shikama , Member, IEEE, Yoshiteru Abe, Toshiki Kishi , Member, IEEE, Koji Takeda , Senior Member, IEEE, Takuro Fujii , Member, IEEE, Hidetaka Nishi , Member, OSA, Takashi Matsui , Atsushi Aratake, Kazuhide Nakajima , Member, IEEE, Member, OSA, and Shinji Matsuo , Fellow, IEEE

Abstract—We describe a new multicore fiber (MCF) receptacle for space division multiplexing (SDM) based transceiver applications, in which we integrated a compact fiber-bundle type fan-in/fan-out device for directly connecting MCF to LDs and PDs. We design the length of the fan-out fibers taking their bending stress into account to achieve a configuration with a smaller footprint. With the proposed receptacle, we develop a 100 Gb/s SDM transmitter based on a four-channel, 1.3 μm membrane laser array on Si, in which spot-size converter (SSC) using inverse taper InP and SiON waveguides is integrated. Since the core size of SiON waveguide is much smaller than that of MCF, we utilize different fibers with optimized modal fields at each connection point and introduce thermally-expanded-core (TEC) fusion splicing to realize a low-loss connection between them. We achieve a pluggable connection between the lasers and 125 μm -cladding 4-core MCF in an LC connector. The developed receptacle maintained satisfactory laser characteristics including sufficient output power and clear eye openings for directly modulated 28 Gb/s NRZ signals. We also achieve an error-free transmission at a bit-error rate of less than 10^{-12} with a 500-m MCF transmission link for all 4 channels with simultaneous 4-channel operation.

Index Terms—Fan-in/fan-out device, multicore fiber (MCF), optical connectors, semiconductor lasers, space division multiplexing (SDM).

I. INTRODUCTION

HIGH-BANDWIDTH optical interconnects are key enablers as regards accommodating the rapid increase in data traffic in the short-/middle-reach links used for data center networks [1]. In such optical interconnects, pluggable transceivers (TRx) including SFP, CFP2, or QSFP are widely

used. They are mainly based on parallel multimode fiber (MMF) transmission with arrays of VCSELs and PDs. Recently, single-mode (SM) transmission with parallel SM fibers (SMF) such as PSM4 [2], or coarse wavelength division multiplexing transmission with (de)multiplexers such as CWDM4 [3] have been introduced to provide higher bandwidth optical interconnects. One promising approach for further increasing the bandwidth density is to combine them with a space division multiplexing (SDM) transmission using multicore fibers (MCFs) and/or few-mode fibers [4]–[7]. Recent demonstrations of SDM for long-haul applications clearly show its effectiveness in terms of overcoming the conventional capacity limits for ultra-large capacity transmission. Such systems also enable us to achieve effective wiring of optical fiber by reducing the number of fibers, or to realize high-density packaging by replacing the MT/MPO connector interface with a small simplex connector interface.

Several demonstrations of end-to-end MCF transmission links for optical interconnect applications have been reported including multi-mode MCF links with 2-dimensional (2-D) VCSEL arrays and PD arrays [8]–[10], and SM-MCF links with silicon (Si) photonics chips with 2-D grating couplers (GCs) [11]–[14]. Both approaches eliminate the need for a fan-in/fan-out (FI/FO) device by using a 2-D coupling arrangement that corresponds to each MCF core. However, issues remain regarding compatibility with the conventional pluggable TRx interface integrated in the package. In addition, GCs still pose challenges in terms of coupling efficiency, wavelength dependence, polarization dependence, and the handling of input/output fibers. On the other hand, an edge coupler such as an inverse taper waveguide [15] can directly couple most existing photonic devices including DFB lasers, modulators, and high-speed detectors to/from an SMF providing a broadband response and a low connection loss with both TE and TM polarization. In this context, realizing a new SM-MCF transmission link based on an edge coupler is also an attractive way to expand SDM TRx applications. To develop such a link, a new optical interface with a FI/FO device is needed to convert the 2-D core arrangement of the MCF to the 1-D core arrangement of the edge couplers. Here, the main challenge we face if we are to realize this interface is to find a way to integrate the FI/FO device with a small footprint accommodated in the TRx package while

Manuscript received September 3, 2018; revised October 23, 2018; accepted October 29, 2018. Date of publication November 1, 2018; date of current version November 28, 2018. (Corresponding author: Kota Shikama.)

K. Shikama, T. Kishi, K. Takeda, T. Fujii, H. Nishi, A. Aratake, and S. Matsuo are with the NTT Device Technology Laboratories, NTT Corporation, Atsugi 243-0198, Japan (e-mail: shikama.kota@lab.ntt.co.jp; toshiki.kishi.ay@hco.ntt.co.jp; koji.takeda.vk@hco.ntt.co.jp; takuro.fujii.uc@hco.ntt.co.jp; hidetaka.nishi.sf@hco.ntt.co.jp; aratake.atsushi@lab.ntt.co.jp; shinji.matsuo.vm@hco.ntt.co.jp).

Y. Abe, T. Matsui, and K. Nakajima are with the NTT Access Network Service Systems Laboratories, NTT Corporation, Tsukuba 305-0805, Japan (e-mail: abe.yoshiteru@lab.ntt.co.jp; takashi.matsui.uh@hco.ntt.co.jp; kazuhide.nakajima.gr@hco.ntt.co.jp).

Color versions of one or more of the figures in this paper are available online at <http://ieeexplore.ieee.org>.

Digital Object Identifier 10.1109/JLT.2018.2879100

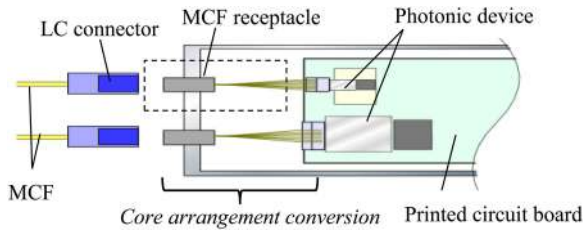


Fig. 1. Schematic diagram of MCF receptacle as optical interface of pluggable transceiver.

keeping the advantages provided by edge couplers. Several types of FI/FO device have been reported including a fiber bundle type [16]–[19], a free space optics type [20] and a direct-written waveguide type [21]. However, these studies have focused solely on how to connect MCF with individual SMFs for long-haul applications and no report had described a FI/FO device integrated with photonic devices for pluggable TRx applications. Against the above background, we have already demonstrated a new MCF receptacle integrated with a FI/FO device [22].

In this paper, expanding on our report in [22], we detail the design and fabrication of an MCF receptacle with a compact FI/FO device for SDM TRx applications. We also provide updated results for a pluggable SDM transmitter consisting of 4-core MCF and 4-channel lasers with our developed receptacle. We then report experimental results for a 500-m transmission link with this configuration for application to short-reach optical interconnects. We describe the successful demonstration of an error-free transmission at a bit-error rate (BER) of less than 10^{-12} for all 4 channels with simultaneous 4-channel operation. The rest of this paper is organized as follows. Section II describes the design guideline of a receptacle for achieving a low connection loss with a small footprint. Section III describes the fabrication of this receptacle for 125- μm cladding diameter 4-core MCF [23] and a 4-channel 1.3 μm membrane laser array on Si (LD-on-Si) [24]–[26]. This section also describes experimental results obtained for the fabricated SDM transmitter with the receptacle including output power versus injected current, excess coupling loss, return loss, and core-to-core XT. Section IV reports the 500-m transmission results we obtained with the devised transmitter, and describes such transmission characteristics as eye diagrams and BERs for directly modulated 25- and 28-Gbps NRZ signals. We offer our conclusions in Section V.

II. DESIGN OF FAN-IN/ FAN-OUT INTEGRATED RECEPTACLE

A. Basic Configuration of Receptacle

Fig. 1 shows a schematic diagram of our proposed receptacle for pluggable TRx applications, where photonic devices for use as an optical transmitter and a detector with edge couplers are integrated in a package. Each photonic device can be integrated with a driver and a trans-impedance amplifier. Moreover, they can be electrically connected to a printed circuit board via subcarriers or interposers by such methods as wire bonding, flip-chip interconnection, and a ball grid array. By plugging a simplex connector with the MCF into this receptacle, we can

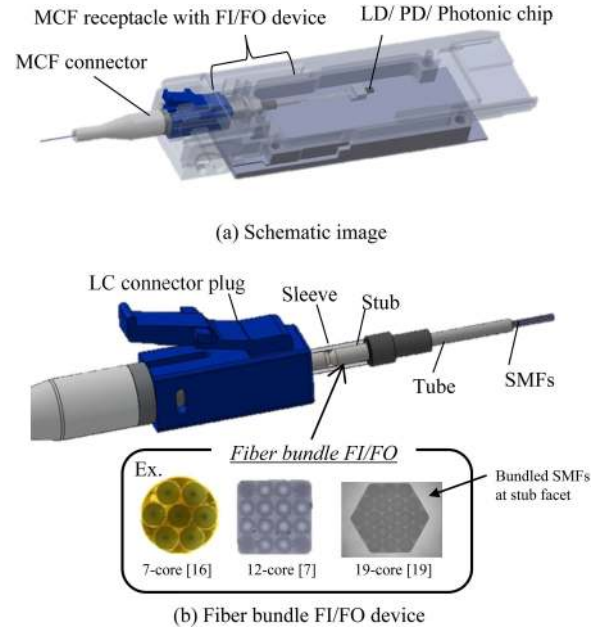


Fig. 2. Basic configuration of our MCF receptacle.

easily achieve optical coupling between a photonic device and the MCF without any specialized equipment, and thus we can construct an SDM transmission link. On this platform, we can use any transmitters and detectors as the photonic devices including a DFB laser array, a modulator array, a Ge/InGaAs photodetector array, and a Si-photonics chip where the laser array, the modulator array, and the detector array are integrated. Here, as described in the previous section, FI/FO devices are needed to convert the core pitch from that of the MCF (mainly with a 2-D array) to the 1-D array of edge couplers. For pluggable TRx applications, the fiber bundle type FI/FO device has advantages over other FI/FO type devices because this type originally uses a connector interface to achieve pluggable and physical-contact (PC) connection. In addition, the fiber-bundle type can yield good optical properties with a small footprint and offers a lot of design flexibility as regards, for example, fiber type, fiber length, and the mounting positions of the photonic devices. Thus, we designed our receptacle based on fiber bundle technologies for TRx applications.

B. Core Arrangement Conversion

Fig. 2 shows the basic configuration of our proposed MCF receptacle integrated with a fiber bundle type FI/FO device, which consists of an LC-compatible stub, a tube, a split sleeve, and an LC connector with an MCF. Here small-diameter SMFs are closely packed in a micro-hole in the stub, where each position of SMF core corresponds to each core of the MCF. The bundled SMFs are expanded through the tube, and their core arrangement changes from a 2-D array to a 1-D one, and they are fixed in place on the opposite side with a glass block. The ends of the ferrule and the stub are appropriately polished to achieve PC connection for all the cores [27]. The LC connector with an MCF is customized with a rotational alignment structure [28]

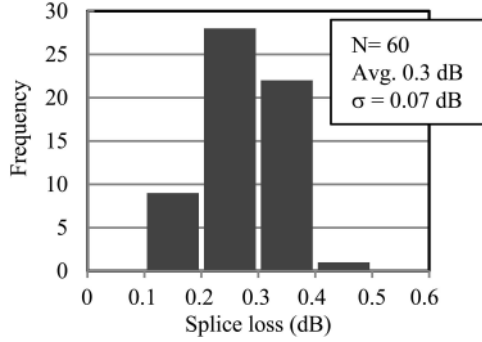


Fig. 3. Histogram of splice loss for TEC fusion splicing between HNAF and SMF.

to align the core position by rotating the ferrule with a flange, and the rotational angle of the MCF is fixed with adhesive once the alignment is completed. The end of the glass block with the fiber array is also polished appropriately for butt-coupling with the photonic device by employing edge couplers. Since the fiber-bundle type can support up to 19-core MCFs with a circular, square, or hexagonal micro-hole as shown in Fig. 2, this receptacle can potentially support up to 19-core MCF with the same structure.

C. Mode-Field Matching Technology

Although the mode-field diameter (MFD) of an edge coupler, such as an inverse taper spot-size converter, can be stably enlarged to about 3–4 μm , there is a large mismatch between its MFD and that of MCF of about 8–10 μm , and thus a large coupling loss occurs. To minimize the coupling loss at each connection point, we use different SMFs in our receptacle. One is an SM high numerical aperture (HNA) fiber with an MFD of about 4 μm for coupling a photonic device employing the edge coupler. The other is a conventional SMF for coupling the MCF. In addition, thermally expanded core (TEC) fusion splicing [29] is performed between these two SMFs to reduce the splicing loss. Fig. 3 shows a histogram of the TEC fusion splicing loss we experimentally performed between an HNA fiber and a conventional SMF with an optimized condition as described in [29] whose cladding diameters are both 80 μm . As shown in Fig. 3, the splicing loss was successfully reduced to an average value of less than 0.3 dB. Thus, by introducing the two SMFs and TEC fusion splicing, we can minimize the excess coupling loss caused by the MFD mismatch, which is the big advantage of our FI/FO device. We can also use tapered fibers as the bundled fibers instead of splicing two different SMFs. The tapered fibers could make the receptacle easier to produce if we can achieve cladding reduction and spot-size conversion simultaneously.

D. Fiber Length Between Each Connection Points

Although the actual mounting positions of the photonic devices in the package depend on the overall design of the TRx configuration including the high-frequency circuits and other components, determining the footprint limit of our receptacle

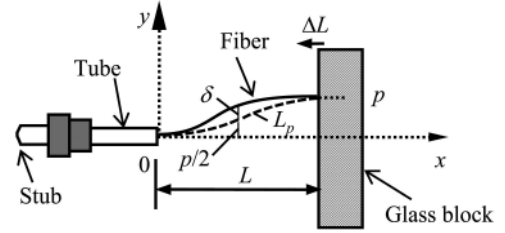


Fig. 4. Schematic model of fiber buckling.

will be a major issue. The footprint of the receptacle is mainly determined by the length of the fan-out fibers between the tube and the glass block. Here, the length limit of these fibers can be designed by calculating the bending stress of them. Fig. 4 shows a schematic diagram of the fibers in the receptacle. In Fig. 4, extra fiber length ΔL is needed to overcome the problem of a lack of length when constructing the receptacle. In addition, the fibers with extra length between the tube and the glass block can cope with variations in their relative positions caused by changes in temperature, which is another advantage of the fiber bundle type FI/FO device. The bending curve shape of the fiber is approximately expressed as [30],

$$y = \frac{\delta}{2} \left(1 - \cos \frac{2\pi x}{L} \right) + \frac{p}{2\pi} \left(\frac{2\pi x}{L} - \sin \frac{2\pi x}{L} \right), \quad (1)$$

where δ , L , and p are deflection, initial length between the tube and the glass block, and the fiber pitch of the fiber furthest from the center of the glass block, respectively. The relationship between δ and ΔL can be calculated from

$$L_p + \Delta L = \int_0^L \sqrt{1 + \left(\frac{dy}{dx} \right)^2} dx, \quad (2)$$

where L_p is the initial bent fiber length caused by pitch conversion. The minimum curvature radius of the fiber can also be calculated from Eq. (1) as follows

$$R_{\min} \approx \frac{L^2}{2\pi^2 \sqrt{\delta^2 + (p/\pi)^2}}. \quad (3)$$

In addition, the maximum bending stress of the bent fiber, σ_{\max} can be calculated as follows

$$\sigma_{\max} = \frac{Ed}{2R_{\min}}, \quad (4)$$

where E and d are Young's modulus ($=76$ GPa) and the cladding diameter of the fiber, respectively. By comparing the maximum bending stress from Eq. (4) with the fiber's maximum tensile stress ($=4.8$ GPa) with certain safety factors, we can determine the minimum fiber length taking the designed extra fiber length into consideration. Since small diameter fibers are better for a compact FI/FO device as described in Eq. (4), we used fibers with an 80 μm cladding diameter. Fig. 5 shows the calculated relationship between the length L and extra fiber length ΔL with different pitches, p . If we take a margin extra length of 100 μm for example, the fiber length must be larger than 5.6 mm with a pitch of 0.375 mm (4-channels with a 250 μm pitch). We can

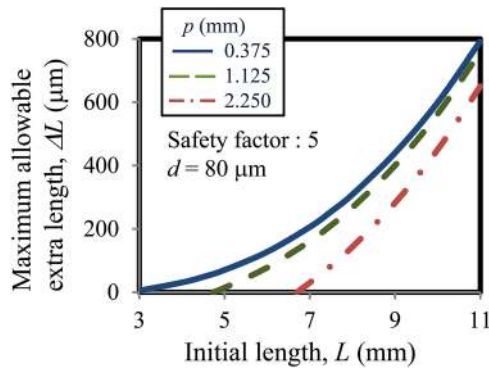


Fig. 5. Relation between initial length and maximum allowable extra length for fiber bundle FI/FO considering tensile stress with a safety factor of 5.

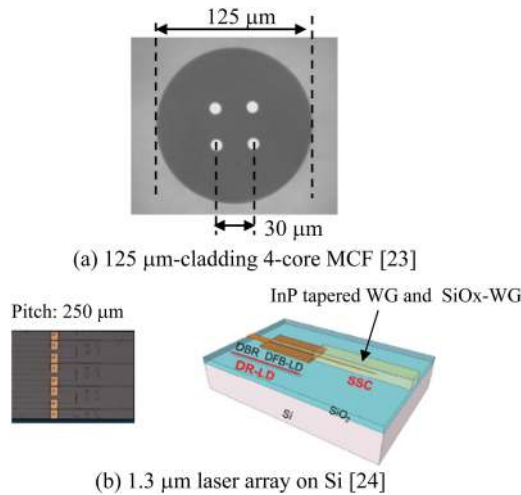


Fig. 6. Devices we used for our receptacle.

also estimate the radiation loss of the bent fiber by calculating the line integral of the power attenuation coefficient along the curved shape of the fiber [31]. Based on these calculations, we can clarify the design guideline regarding the fiber length for the receptacle.

III. RECEPTACLE INTEGRATION WITH LASER ARRAY

A. Device Configuration

As a case study, we devised an MCF receptacle with our compact FI/FO device for 125- μm cladding diameter MCF. Fig. 6(a) shows a cross-sectional view of the 4-core MCF [23] that we used in our study. The cladding diameter of the MCF is 125 μm and the MFD is about 7.6 μm at a wavelength of 1.3 μm . The core pitch is about 30 μm and the designed SM cut-off wavelength is 1.19 μm . The 125 μm cladding diameter MCF is suitable for optical interconnect applications because we can handle it with the same flexibility as conventional 125 μm -cladding SMF. In addition, the 125- μm MCF is promising for use as the first practical MCF because it also allows us to achieve mass-productivity and to use standard fiber components including optical connectors and cable [32], [33].

As a photonic device for this study, we used a four-channel, 1.3 μm membrane laser array on Si (LD-on-Si) [24]. An LD-on-

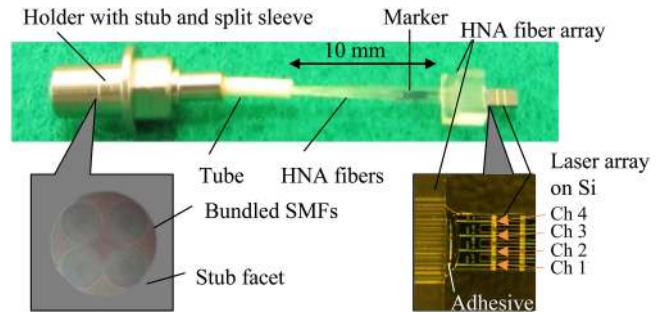


Fig. 7. Fabricated MCF receptacle for connecting 4-core MCF with laser array on Si.

Si is a promising candidate as a future ultra-low power consumption transmitter for short- to middle-reach applications. The LD-on-Si was successfully developed by the epitaxial growth of six InGaAlAs based QW layers on an InP-SOI substrate whose core pitch was 250 μm , as shown in Fig. 6(b). This device was also integrated with a spot-size converter using an inverse taper InP and a SiON core as an edge coupler, which allow us to directly couple the SM HNA fiber with a low coupling loss.

B. Receptacle Fabrication

On the basis of the principles described in the previous section, we then fabricated the receptacle for the 4-core MCF and 4-channel LD-on-Si. Fig. 7 shows the fabricated receptacle. The fabrication process was as follows. First, we performed TEC fusion splicing between an SMF and an HNA fiber under the same conditions as those described in Fig. 3. Next, the cladding of the SMFs was reduced to almost the same value as the core pitch of the MCF by chemical etching. They were then inserted into a circular micro-hole in the stub with a tube. Here, the point at which TEC fusion-splicing was performed was accommodated in the stub to protect the splicing point properly without a polymer coating. The SMFs were then fixed in place with adhesive and the end of the stub was polished so that it became spherical to achieve PC connection for all 4 cores. As shown in Fig. 7, the bundled SMFs were closely packed where each core corresponds to each core of the MCF. Then, the stub was integrated in the metal holder, and the rotational angle of the stub was aligned and fixed in place by inserting the rotational LC connector with the MCF into the stub and aligning it with the active alignment method. Next, the HNA fibers on the opposite side were assembled in a glass block with V-grooves whose pitch was about 250 μm . The HNA fiber length L was set at 10 mm in our work taking account of the bending stress including certain margins where the bending losses of HNA fibers are negligible thanks to the HNA fiber's low radiation loss. We polished a facet of the glass block and then butt-coupled it to the LD-on-Si with the active alignment method and fixed it in place with adhesive. Fig. 8 shows the assembled receptacle housed in a QSFP-based dummy package, where an LC connector with the MCF was inserted. We confirmed that the fabricated receptacle could be accommodated in the QSFP package for an optical interface.

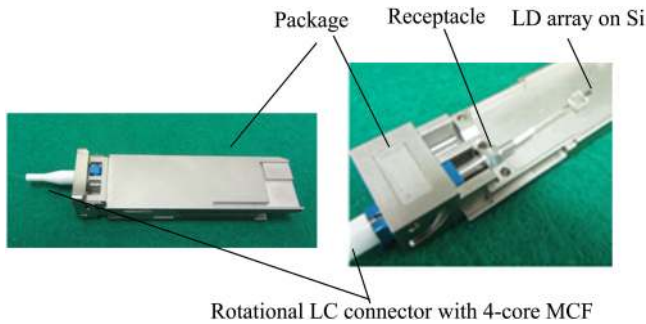


Fig. 8. Receptacle in QSFP based dummy package.

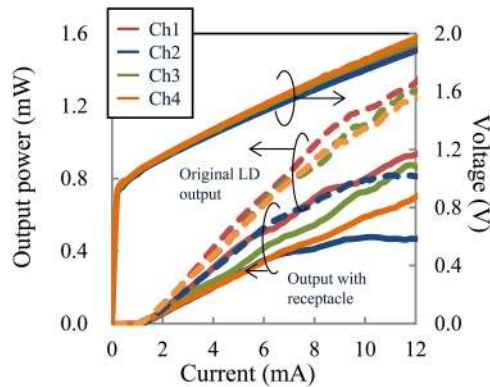


Fig. 9. Output powers and applied voltages versus injected current before and after connection of fabricated receptacle with 10-m MCF including two FI/FOs.

TABLE I
ESTIMATED LOSS BREAKDOWN OF FABRICATED RECEPTACLE WITH 10-M
MCF AT BIAS CURRENT OF 10 MA

Cause of Loss (Unit: dB)	Ch1	Ch2	Ch3	Ch4
Total excess loss	1.6	2.2	1.8	2.6
Loss between MCF and SMFs with another FI/FO	0.5	0.5	0.7	0.8
Loss between MCF and HNA fibers with our receptacle	0.5	0.5	0.8	0.7
Loss between LD-on-Si and HNA fiber array	0.6	1.2	0.3	1.1

C. Optical Properties

We measured the output power of the LD-on-Si as a function of the injected current via the fabricated receptacle, which was connected to the LC connector with 10-m long MCF, for a back-to-back configuration. Here, we also used another fiber bundle type FI/FO device to measure each channel that was transmitted through each core of the MCF. We also measured the output power of the LD-on-Si via the HNA fiber as a reference. Then, we estimated the excess coupling loss by measuring the output power change before and after the insertion of the receptacle with the MCF. Fig. 9 shows the output powers and applied voltages as a function of injected bias current. The average output power through the MCF was -2.1 dBm at a bias current of 10 mA, and the power consumption was extremely small thanks to the LD-on-Si.

Table I shows the loss breakdown of the receptacle estimated by measuring the optical losses prior to assembly. The average and maximum excess losses were 1.4 and 1.8 dB, respectively,

without another FI/FO device. The total average excess loss of the configuration was 2.0 dB. Here, the losses at the FI/FO device connection mainly depended on the offset misalignment of each core, which can be reduced by improving the core position accuracy of the MCF and the bundled SMFs in the micro-hole. Moreover, the losses that occurred at the connection between the LD-on-Si and the HNA fibers mainly depended on the pitch errors in the V-groove and can be reduced by improving these pitch errors. Then, we measured the return losses at the connection point between the FI/FO device and the LC connector with an optical low-coherence reflectometer. We confirmed that all the cores provided sufficiently high return losses of more than 40 dB, which indicates that PC connections were successfully achieved. The optical crosstalk for 4-channel simultaneous operation was confirmed to be less than -50 dB with this configuration.

IV. MCF TRANSMISSION RESULTS WITH RECEPTACLE

A. Direct Modulation Characteristics

To evaluate the transmission characteristics with this transmitter configuration, we then connected a 500-m-long 4-core MCF with the developed receptacle by plugging another LC connector with a 500-m MCF into the receptacle. The measured splicing losses and transmission losses of the 500-m MCF totaled from 0.3 to 1.1 dB. With both the devised 500-m-long MCF transmission link and the previous back-to-back configuration, we then demonstrated 25- and 28-Gbit/s direct modulation with the NRZ signals. Fig. 10 shows the experimental setup that we used for measuring the lasing spectra, eye diagrams, and BER after the transmission. Fig. 11 shows the measured lasing spectra transmitted through the 500-m MCF during the simultaneous operation of a 4-channel LD-on-Si at a bias current of 10 mA. As shown in Fig. 11, there was little difference between each emission wavelength, which is considered to be caused by LD-on-Si fabrication errors. We observed a crosstalk of about -40 dB, which was caused by the core-to-core crosstalk of the 500-m-long 4-core MCF although the effect of these crosstalk values was negligible as regards the transmission characteristics.

Fig. 12 shows the measured average output power, P_{avg} and eye diagrams when each laser was simultaneously modulated for 28-Gbps NRZ signals at 25 °C for a back-to-back transmission and the 500-m MCF transmission link. In Fig. 12, each input signal amplitude was $0.6 V_{\text{pp}}$ at a bias current of 10 mA and all the modulations were loaded using a pseudo-random bit sequence (PRBS) of $2^{31} - 1$ via a 4-channel probe. As shown in Fig. 12, each channel operates with clear eye openings for both 25- and 28-Gbps NRZ signals with an extinction ratio of about 4-5 dB. This indicates that our receptacle maintains sufficiently good LD characteristics without such degradations as optical reflections.

B. BER Characteristics

We then measured the BER for the 500-m MCF transmission link with our receptacle. The operating conditions were the same as for the eye diagram measurement described in Fig. 12. Fig. 13 shows the measured BER characteristics for back-to-back and

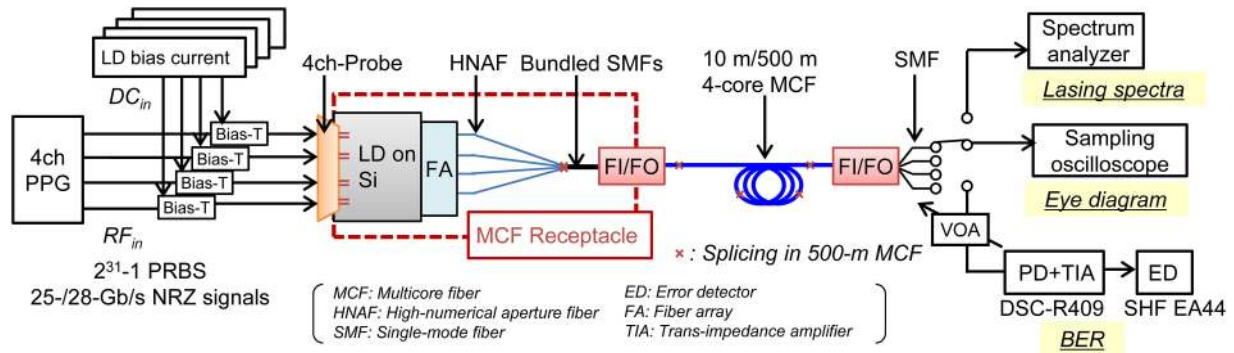


Fig. 10. Experimental setup.

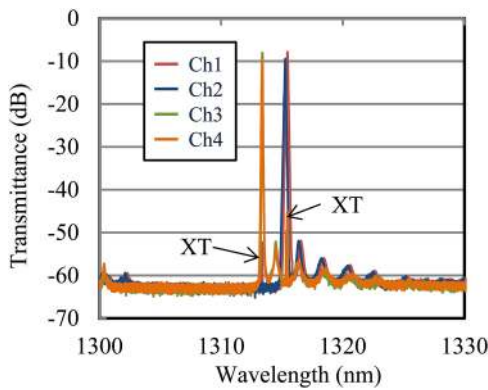


Fig. 11. Lasing spectra with 500-m MCF including FI and FO during the simultaneous operation of 4-channel lasers at a bias current of 10 mA.

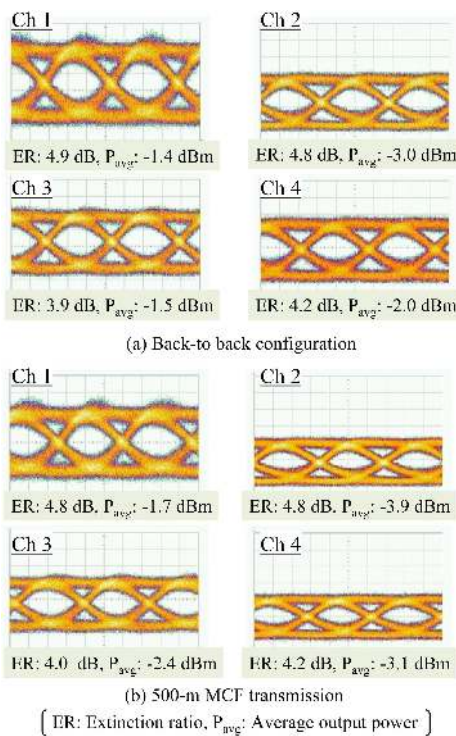
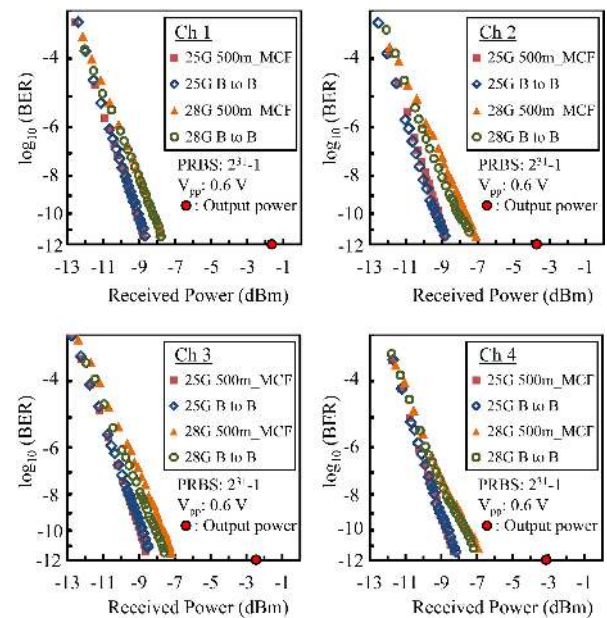
Fig. 12. Eye diagrams for (a) back-to-back configuration and (b) 500-m MCF transmission when all channels were operated simultaneously with 28-Gbps NRZ signals at a bias current of 10 mA. Each input signal amplitude was 0.6 V. (Horizontal axis scale: 10 ps/div, Vertical axis scale: 300 μ W/div.)

Fig. 13. Bit-error-rate characteristics of developed SDM transmitter. Each BER was measured during the simultaneous operation of 4-channel lasers at a bias current of 10 mA.

500-m MCF transmission configurations. As shown in Fig. 13, there were margins of more than about 4 dBm between the fiber output power and the minimum receiver sensitivity for each channel. Moreover, we confirmed that error-free transmissions at a BER of less than 10^{-12} over a 500-m-long MCF were successfully achieved for all the channels during the simultaneous operation. These results indicate that our receptacle is applicable to a 100-Gbps transmission link with a 500-m-long (or longer) MCF, and that it maintains sufficient transmitter quality for optical interconnect applications.

V. CONCLUSION

We developed the first MCF receptacle as a new optical interface for SDM TRx applications. Our receptacle is compatible with the LC connector used for a conventional pluggable TRx package. We designed the receptacle based on a fiber bundle type FI/FO device so that we could connect each core of the MCF to the photonic device with a small footprint. With the

receptacle, we introduced two different fibers and employed TEC fusion splicing to minimize the connection loss between the MCF and such photonic devices employing an edge coupler as PDs or LDs. We then devised the receptacle for use with 125- μm cladding 4-core MCF and a 1.3 μm , 4-channel LD-on-Si for a next-generation ultra-low power consumption transmitter. We successfully connected the components and realized good optical performance including a low excess coupling loss and directly modulated 28 Gbps NRZ operation (PRBS: $2^{31}-1$) with clear eye openings. We also successfully demonstrated an error-free transmission at a bit-error rate of less than 10^{-12} with a 500-m MCF transmission link for all 4 channels with simultaneous 4-channel operation. The results revealed the potential of 100 Gbps MCF transmission links with our developed receptacle. The receptacle can be applied to pluggable SDM TRx applications, and also to on-board optics with future SDM transmission links.

REFERENCES

- [1] C. Kachris and I. Tomkos, "A survey on optical Interconnects for data centers," *IEEE Commun. Surveys Tuts.*, vol. 14, no. 4, pp. 1021–1036, Jan.–Mar. 2012.
- [2] 100G PSM4 Specification Version 2.0., Sep. 2014. [Online]. Available: <http://www.psm4.org/>
- [3] 100G CWDM4 MSA technical specifications rev 1.0., Aug. 2014. [Online]. Available: <http://www.cwdm4-msa.org/>
- [4] T. Morioka, Y. Awaji, R. Ryf, P. Winzer, D. Richardson, and F. Poletti, "Enhancing optical communications with brand new fibers," *IEEE Comput. Mag.* vol. 50, no. 2, pp. S31–S42, Feb. 2012.
- [5] H. Takara *et al.*, "1.01-Pb/s (12 SDM/222 WDM/456 Gb/s) Crosstalk-managed transmission with 91.4-b/s/Hz aggregate spectral efficiency," presented at the Eur. Conf. Exhib. Opt. Commun., Amsterdam, The Netherlands, 2012, Paper Th.3.C.1.
- [6] R. Ryf *et al.*, "Space-division multiplexing over 10 km of three-mode fiber using coherent 6×6 MIMO processing," presented at the Opt. Fiber Commun. Conf. Exhib., Los Angeles, CA, USA, 2011, Paper PDPB10.
- [7] T. Mizuno *et al.*, "12-core \times 3-mode dense space division multiplexed transmission over 40 km employing multi-carrier signals with parallel MIMO equalization," presented at the Opt. Fiber Commun. Conf., San Francisco, CA, USA, 2014, Paper Th5B.2.
- [8] B. Zhu, T. F. Taunay, M. F. Yan, M. Fishteyn, G. Oulundsen, and D. Vaidya, "70-Gb/s multicore multimode fiber transmissions for optical data links," *IEEE Photon. Technol. Lett.*, vol. 22, no. 22, pp. 1647–1649, Nov. 2010.
- [9] B. G. Lee *et al.*, "End-to-end multicore multimode fiber optic link operating up to 120 Gb/s," *IEEE J. Lightw. Technol.*, vol. 30, no. 6, pp. 886–892, Mar. 2012.
- [10] F. E. Doany *et al.*, "Multicore fiber 4TX + 4RX optical transceiver based on holey SiGe IC," presented at the IEEE 64th ECTC, Lake Buena Vista, FL, USA, 2014, pp. 1016–1020.
- [11] T. Pinguet *et al.*, "Silicon photonics multicore transceivers," presented at the IEEE Photon. Soc. Summer Topical Meeting Series, Seattle, WA, USA, 2012, Paper WC4.1.
- [12] C. R. Doerr and T. F. Taunay, "Silicon photonics core-, wavelength-, and polarization-diversity receiver," *IEEE Photon. Technol. Lett.*, vol. 23, no. 9, pp. 597–599, Mar. 2011.
- [13] P. D. Heyn *et al.*, "Ultra-Dense 16×56 Gb/s NRZ GeSi EAM-PD arrays coupled to multicore fiber for short-reach 896 Gb/s optical links," presented at the Opt. Fiber Commun. Conf. Exhib., Los Angeles, CA, USA, 2017, Paper M3G.3.
- [14] T. Hayashi *et al.*, "End-to-end multi-core fibre transmission link enabled by silicon photonics transceiver with grating coupler array," presented at the Eur. Conf. Opt. Commun., 2017, Paper Th.2.A.4.
- [15] T. Shoji, T. Tsuchizawa, T. Watanabe, K. Yamada, and H. Morita, "Low loss mode size converter from 0.3 μm square si wire waveguides to single mode fibres," *Electron. Lett.*, vol. 38, no. 2, pp. 1669–1670, 2002.
- [16] Y. Abe, K. Shikama, S. Yanagi, and T. Takahashi, "Physical-contact-type fan-out device for multicore fibre," *Electron. Lett.*, vol. 49, no. 11, pp. 711–712, 2013.
- [17] K. Watanabe, T. Saito, K. Imamura, and M. Shiino, "Development of fiber bundle type fan-out for multi-core fiber," presented at the Opt. Electron. Commun. Conf., Busan, South Korea, 2012, pp. 475–476.
- [18] Y. Abe, K. Shikama, H. Ono, S. Yanagi, and T. Takahashi, "Fan-in/fan-out device employing v-groove substrate for multicore fibre," *Electron. Lett.*, vol. 51, no. 17, pp. 1347–1348, 2015.
- [19] K. Shikama, Y. Abe, H. Ono, and A. Aratake, "Low-loss and low-mode-dependent-loss fan-in/fan-out device for 6-mode 19-core fiber," *IEEE J. Lightw. Technol.*, vol. 36, no. 2, pp. 302–308, Jan. 2018.
- [20] W. Klaus *et al.*, "Free-space coupling optics for multicore fibers," *IEEE Photon. Technol. Lett.*, vol. 24, no. 11, pp. 1902–1905, Nov. 2012.
- [21] R. R. Thomson *et al.*, "Ultrafast-laser inscription of a three dimensional fanout device for multicore fiber coupling applications," *Opt. Express*, vol. 15, no. 18, pp. 11691–11697, 2007.
- [22] K. Shikama *et al.*, "Multicore-fiber LC receptacle with compact fan-in/fan-out for short-reach transceivers," presented at Opt. Fiber. Commun. Conf. Exhib., San Diego, CA, USA, 2018, Paper W1A.7.
- [23] T. Sakamoto, T. Mori, M. Wada, T. Yamamoto, T. Matsui, K. Nakajima, and F. Yamamoto, "Experimental and numerical evaluation of inter-core differential mode delay characteristic of weakly-coupled multi-core fiber," *Opt. Express*, vol. 22, no. 26, pp. 31966–31976, 2014.
- [24] T. Fujii *et al.*, "1.3- μm directly modulated membrane laser array employing epitaxial growth of InGaAlAs MQW on InP/SiO₂/Si substrate," presented at the Eur. Conf. Opt. Commun., Düsseldorf, Germany, 2016, Paper Th.3.A.2.
- [25] H. Nishi *et al.*, "Membrane distributed-reflector laser integrated with SiO_x-based spot-size converter on si substrate," *Opt. Express*, vol. 24, no. 16, pp. 18346–18352, 2016.
- [26] T. Kishi *et al.*, "A 137-mW, 4 ch \times 25-gbps low-power compact transmitter flip-chip-bonded 1.3- μm LD-array-on-Si," presented at Opt. Fiber Commun. Conf. Exhib., San Diego, CA, USA, 2018, Paper M2D.2.
- [27] K. Shikama, Y. Abe, S. Yanagi, and T. Takahashi, "Physical-contact conditions for multicore fiber optical connectors," presented at the Opt. Fiber Commun. Conf. Exhib., Anaheim, CA, USA, 2013, Paper OM3I.1.
- [28] K. Shikama, Y. Abe, S. Yanagi, S. Asakawa, and T. Takahashi, "Multicore fiber connector with physical-contact connection," *IEICE Trans. Electron.*, vol. E99.C, no. 2, pp. 242–249, 2016.
- [29] T. Oda, K. Hirakawa, K. Ichii, S. Yamamoto, and K. Aikawa, "Thermally expanded core fiber with a 4-mm mode field diameter suitable for low-loss coupling with silicon photonic devices," presented at the Opt. Fiber Commun. Conf. and Exhib., San Francisco, CA, USA, 2017, Paper Tu3K.5.
- [30] S. P. Timoshenko and J. M. Gere, *Theory of Elastic Stability*, 2nd ed. New York, NY, USA: McGraw-Hill, 1961.
- [31] M. Kobayashi, S. Asakawa, R. Nagase, and S. Mitach, "A new physical contact connection method using the buckling force of optical fiber," *IEICE Trans. Electron.*, vol. E80.C, no. 2, pp. 334–339, 1997.
- [32] T. Matsui *et al.*, "Design of 125 μm cladding multi-core fiber with full-band compatibility to conventional single-mode fiber," presented at the Eur. Conf. Opt. Commun., Valencia, Spain, 2015, Paper We.1.4.5.
- [33] T. Matsui *et al.*, "118.5 Tbit/s transmission over 316 km-long multi-core fiber with standard cladding diameter," presented at the Opto-Electronics Commun. Conf. Photon. Global Conf., Singapore, 2017, Paper PD2.

Kota Shikama (M'14) received the B.E. and M.E. degrees in materials science from Keio University, Kanagawa, Japan, in 2008 and 2010, respectively. He joined the NTT Photonics Laboratories, Atsugi, Kanagawa, Japan, in 2010. He has been conducting research on optical packaging technologies for space division multiplexing components and high port-count wavelength selective switches. He received the Young Award from the IEEE Components, Packaging and Manufacturing Technology Symposium Japan in 2012. He received the Young Engineer Award from the Institute of Electronics, Information and Communication Engineers (IEICE) of Japan in 2013. He is a Member of the IEICE.

Yoshiteru Abe received the B.E. degree in electrical engineering, the M.E. degree in electronic device engineering, and the Dr. Eng degree in electrical engineering from Kyushu University, Fukuoka, Japan, in 1996, 1998, and 2005, respectively. In 1998, he joined the Nippon Telegraph and Telephone Corporation Optoelectronics Laboratories, Atsugi, Kanagawa, Japan. He is currently with the Access Network Service Systems Laboratories, NTT Corporation, Tsukuba, Ibaraki, Japan. His research interests include optical fiber connectors.

Toshiki Kishi (M'13) received the B.E. and M.E. degrees in electrical engineering from the Tokyo University of Science, Tokyo, Japan, in 2011 and 2013, respectively. In 2013, he joined NTT Photonics Laboratories, NTT Corporation, Kanagawa, Japan, where he has been engaged in research and development of ultrahigh-speed mixed signal ICs for optical communications systems. He is currently with NTT Device Technology Laboratories, Kanagawa, Japan. He is a Member of the Institute of Electronics, Information and Communication Engineers of Japan.

Koji Takeda (S'06–M'10–SM'16) received the B.S., M.S., and Ph.D. degrees in electronics engineering from the University of Tokyo, Tokyo, Japan, in 2005, 2007, and 2010, respectively. From 2008 to 2010, he received research fellowship for young scientists from Japan Society for the Promotion of Science. In 2010, he joined NTT Photonics Laboratories. His current research interests include ultralow-power optical interconnect, InP photonic integrated circuit, and photonic crystal lasers. He is a Member of the IEICE and the JSAP. He received the Best Student Paper Award from IEEE Photonics Society in 2009 and the Outstanding Student Presentation Award from JSAP in 2010.

Takuro Fujii (M'18) received the B.E. and M.E. degrees in system design engineering from Keio University, Kanagawa, Japan, in 2010 and 2012, respectively. In 2012, he joined NTT Photonics Laboratories, Atsugi, Japan. He has been researching MOVPE growth of III–V semiconductors and the development of III–V semiconductor lasers on Si for photonic integrated circuits. He is a Member of Institute of Electronics, Information and Communication Engineers (IEICE) and Japanese Society of Applied Physics (JSAP). He received the Young Scientist Presentation Award from the JSAP in 2014.

Hidetaka Nishi received the B.E. and M.E. degrees in mechanical science and engineering and the Ph.D. degree in electronics and applied physics from Tokyo Institute of Technology, Tokyo, Japan, in 2005, 2007, and 2016, respectively. In 2007, he joined NTT Microsystem Integration Laboratories. Since then he has been conducting research on integrated photonic and plasmonic devices. He is a Member of the Optical Society of America (OSA) and JSAP.

Takashi Matsui received the B.E., M.E., and Ph.D. degrees from Hokkaido University, Sapporo, Japan, in 2001, 2003, and 2008, respectively, all in electronic engineering. He also attained the status of Professional Engineer (P.E.Jp) in electrical and electronic engineering in 2009. In 2003, He joined NTT Access Network Service Systems Laboratories, Ibaraki, Japan. He has been engaged in research on optical fiber design techniques. He is a Member of the Institute of Electronics, Information and Communication Engineers (IEICE) of Japan.

Atsushi Aratake received the B.E. and M.E. degrees in nuclear engineering from Kyoto University, Kyoto, Japan, in 1995 and 1997, respectively. He joined NTT System Electronics Laboratories, Atsugi, Japan, where he undertook research on advanced interconnection for ultrahigh-speed devices. From 2004 to 2007, he was involved in research on the reliability of PLC-type optical components at NTT Photonics Laboratories, Atsugi. In 2007, he moved to the Research and Development Planning Department, Tokyo, Japan, where he is involved in project and resource management for NTT R&D. From 2010 to 2011, he was with NTT Photonics Laboratories, Atsugi, where he developed assembly technologies for silica-LiNbO₃ hybrid modulators and 100-Gb/s optical receiver front-end modules. He is currently a Senior Research Engineer, Supervisor at NTT Device Technology Laboratories, Atsugi, and a Senior Member of the Institute of Electronic, Information and Communication Engineers (IEICE) of Japan.

Kazuhide Nakajima (M'05) received the M.S. and Ph.D. degrees in electrical engineering from Nihon University, Chiba, Japan, in 1994 and 2005, respectively. In 1994, he joined NTT Access Network Systems Laboratories, Tokai, Ibaraki, Japan, where he engaged in research on optical fiber design and related measurement techniques. He is currently a Senior Research Engineer, Supervisor (Senior Distinguished Researcher), and a Group Leader at NTT Access Network Service Systems Laboratories, Tsukuba, Ibaraki, Japan. He is also acting as Rapporteur Q5/SG15 of ITU-T. He is a Member of the Institute of Electronics, Information and Communication Engineers (IEICE) and the Optical Society of America.

Shinji Matsuo (M'95–SM'14–F'16) received the B.E. and M.E. degrees in electrical engineering from Hiroshima University, in 1986 and 1988, and the Ph.D. degree in electronics and applied physics from Tokyo Institute of Technology, in 2008. In 1988, he joined NTT Optoelectronics Laboratories, where he researched photonic functional devices using multiple quantum well pin modulators and VCSELs. In 1997, he researched optical networks using WDM technologies at NTT Network Innovation Laboratories. Since 2000, he has been researching high-speed tunable optical filters and lasers at NTT Photonics Laboratories and NTT Device Technology Laboratories.

Dr. Matsuo is a Senior Distinguished Researcher of NTT. He is a Member of the JSAP and IEICE.